

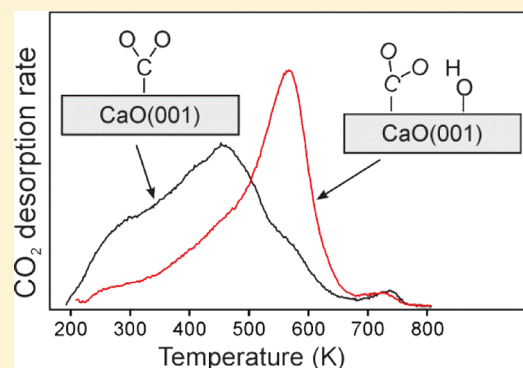
CO₂ Adsorption on CaO(001): Temperature-Programmed Desorption and Infrared Study

Xuefei Weng,[†] Yi Cui,[‡] Shamil Shaikhutdinov,^{*†} and Hans-Joachim Freund[‡]

Abteilung Chemische Physik, Fritz-Haber-Institut der Max-Planck-Gesellschaft, Faradayweg 4-6, 14195 Berlin, Germany

Supporting Information

ABSTRACT: We studied adsorption of CO₂ on well-ordered thin CaO(001) films, prepared on Mo(001) and Pt(001) single-crystal surfaces in ultrahigh vacuum (UHV) conditions, using infrared reflection-absorption spectroscopy (IRAS) and temperature-programmed desorption (TPD). At low coverages, CO₂ adsorbs as monodentate carbonates (CO₃²⁻). TPD spectra showed pseudo-first-order desorption kinetics with a maximum shifting from 500 to 470 K with increasing CO₂ coverage. However, at further increasing exposures, desorption maximum is shifted to the considerably higher temperatures (570 K), although CO₂ uptake remained almost the same. This unusual effect was found to correlate with dissociative adsorption of residual water in the UHV background as observed both by TPD and IRAS. Comparative analysis of spectral evolution on crystalline CaO(001) films and CaO nanoparticles favors the model, where surface hydroxyls only affect adsorption geometry of the carbonates rather than form bicarbonate species. However, hydroxyls show stabilizing effect on CO₂ binding to the CaO surface.



1. INTRODUCTION

Carbon dioxide (CO₂) is an abundant chemical feedstock with wide applications in industry. Driven by growing energy and environmental concerns, capturing/sequestering of CO₂ has recently received enormous attention.¹ In this respect, alkaline-earth oxides such as calcium oxide (CaO) were found as promising materials: they are abundant in nature, low-cost, and exhibit high CO₂ uptake and good thermal stability.^{2–4}

Adsorption and reactivity studies on CaO were primarily performed on powders. Complete adsorption of CO₂ results in the formation of calcium carbonate (CaCO₃), which was found to occur in two kinetic regimes. There has been great interest in understanding the initial stages of adsorption. In an early infrared spectroscopy study,⁵ the formation of carbonate (CO₃²⁻) species on a CaO surface was proposed as a monodentate at room temperature, with the appearance of bidentate carbonates at higher temperatures. Substantial efforts to understand the IR spectra of CO₂ adsorption on CaO were made via theory. Monodentate carbonates were predicted to form on terrace, edge, and step sites, whereas bidentate carbonates may only be formed on corner sites.^{6,7}

However, full understanding of chemical reactions on CaO surfaces is still missing that renders fundamental studies on well-defined systems a necessity.^{8–10} Experimental studies employing “surface science” methodology remain scarce, mainly because of the difficulties in the preparation of well-defined CaO surfaces as well as high reactivity of CaO toward ambient gases. A synchrotron-based photoemission spectroscopy study of CO₂ adsorption on vacuum-cleaved single-

crystal CaO(001) surfaces showed the formation of a surface carbonate species at pressures above 10⁻⁶ Torr.¹¹ Molecular beam and temperature-programmed desorption (TPD) experiments, performed on a reduced CaO(001) crystal surface, suggested carbonate decomposition to CO.¹² Note, however, that the surface under study showed no clear diffraction pattern that was assigned to high density of defects, presumably oxygen vacancies. Few adsorption studies primarily using photoelectron spectroscopies were performed on CaO thin films grown on Si(111) and Si(001).^{13,14} However, the prepared films were polycrystalline in nature and poorly defined.

In our own laboratories, well-ordered thin films of CaO(001) were prepared on a Mo(001) substrate. Low-energy electron diffraction (LEED) and scanning tunneling microscopy (STM) studies showed films exhibiting properties virtually identical to the bulk,¹⁵ although adventitious Mo segregation at elevated temperatures to the surface has to be controlled.¹⁶ It was shown that the presence of Mo atoms in the sub-surface region may affect surface reactions, in particular with O₂.¹⁷

Infrared reflection-absorption spectroscopy (IRAS) experiments of initial stages of CO₂ adsorption on CaO(001) films showed vibrational modes consistent with surface carbonates.^{18,19} On the basis of theoretical calculations, the IR

Received: November 26, 2018

Revised: December 13, 2018

Published: December 27, 2018

bands were assigned to monodentate carbonate species that first adsorb at steps and other low-coordinate sites, followed by surface islanding of monodentate carbonates adsorbed on terraces.

In the continuation of our previous studies, we performed TPD and IRAS study of CO₂ adsorption on CaO(001) films in a wide range of coverages and exposures. In addition to films grown on Mo(001), here we report preparation of well-ordered CaO(001) films on a Pt(001) substrate, which is thought (as a noble metal) to be more resistant toward surface segregation. The Pt(001) surface has a much shorter lattice constant (≈ 2.77 Å) than does Mo(001) (≈ 3.147 Å), thus resulting in $\sim 20\%$ lattice mismatch to CaO(001) (≈ 3.402 Å). In principle, comparative study of the two systems would allow one to examine the support effects, if any, on the surface chemistry of thin CaO(001) films.

2. METHODS AND MATERIALS

The experiments were performed in several ultrahigh vacuum (UHV) chambers. The first chamber is equipped with four-grid LEED optics (from Specs), also used for Auger electron spectroscopy (AES) measurements, a differentially pumped quadrupole mass spectrometer (QMS, Hiden HAL 301) and an STM (Omicron). The Pt(001) crystal (99.99% from MaTeck GmbH) was mounted on the Omicron sample holder. The sample could be heated by electron bombardment from the backside of the crystal using a tungsten filament. The temperature was measured by a chromel–alumel thermocouple spot-welded at the edge of the crystal. CO₂ (Linde, purity 4.5) was dosed by backfilling the chamber. The heating rate in TPD experiments was 3 K s^{-1} .

The second chamber is equipped with LEED/AES (Specs) and differentially pumped QMS (Hiden HAL 301/3F). The Pt(001) or Mo(001) single crystal (99.99%, both from MaTeck GmbH) was spot-welded to the two Ta wires for resistive heating as well as cooling that is achieved by filling the manipulator rod with liquid nitrogen. The sample temperature was measured by a K-type thermocouple spot-welded to the backside of the crystal. In this setup, CO₂ was dosed by a directional gas doser placed ~ 0.5 mm from the crystal surface.

The third chamber is equipped with LEED, STM, X-ray photoelectron spectroscopy (XPS), and an IR spectrometer (Bruker IFS 66v). The Mo(001) crystal was mounted on an Omicron sample holder, with the temperature measured by a thermocouple at the edge of the crystal. CO₂ was dosed by backfilling the chamber. The IRA spectra were recorded using a p-polarized light at an 84° grazing angle of incidence (spectral resolution 4 cm^{-1}).

In all chambers, the metal surfaces were cleaned by cycles of Ar⁺ ion sputtering and annealing in UHV at high temperatures. Residual carbon was removed by mild oxidation in 10^{-7} mbar O₂ at 700 K and subsequent flash to 1000 K in UHV. The surface cleanliness was checked by LEED and AES (XPS) prior to the Ca deposition performed from a Mo crucible using a commercial evaporator (Omicron EFM 3). Well-ordered CaO(001) films were grown on Mo(001) as described elsewhere.^{15,18}

3. RESULTS

3.1. Preparation of CaO(001) Films on Pt(001). We first address the preparation of CaO(001) thin films on Pt(001). Basically, we made use of the same approach as reported for a

Mo(001) substrate.¹⁵ Ca was vapor-deposited in oxygen ambient (5×10^{-7} mbar O₂) onto the crystal surface kept at 300 K. The resulted CaO overlayer showed no diffraction spots in LEED. Then, the sample was annealed in UHV at elevated temperatures to induce long-range ordering which was monitored by LEED. This typically requires annealing temperatures of 1000 K and above (see Figure S1 in the Supporting Information). Auger spectra revealed no changes in Ca and O peak intensities on stepwise heating from 700 to 1200 K, indicating that annealing solely caused film ordering and does not affect chemical composition (Figure S2 in the Supporting Information).

Figure 1a,b compares LEED patterns of the well-known “hex”-reconstructed Pt(001) surface and the CaO film,

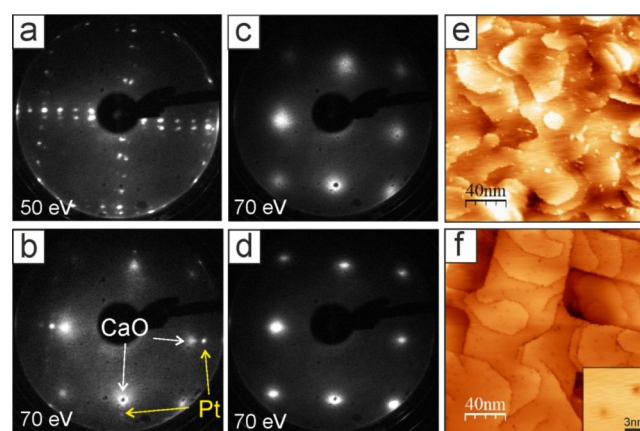


Figure 1. LEED patterns of a clean Pt(001)-hex surface (a) and a sub-monolayer CaO(001) film annealed at 900 K (b) at electron energies as indicated. LEED patterns and STM images of a closed CaO(001)/Pt(001) film annealed in UHV at 1000 K (c,e) and 1150 K (d,f). The inset shows randomly distributed point-like defects imaged as depressions (Tunneling parameters: bias 4.5 V, current 0.1 nA).

partially covering the metal surface. The diffraction spots of CaO are aligned with those of Pt(001)-(1 × 1), thus suggesting epitaxial growth of CaO(001) on Pt(001) despite of a large ($\sim 20\%$) lattice mismatch. Using diffraction spots of Pt(001)-(1 × 1) as a reference, we obtained 3.35 Å for the lattice constant of the prepared CaO(001) films, which is in fairly good agreement with 3.40 Å of CaO(001). However, on further UHV annealing of this sub-monolayer film to 1200 K, the oxide-related spots disappeared and only the Pt(001)-(1 × 1) diffraction spots remained, indicating film decomposition either via sublimation or dissolution into the Pt crystal. Indeed, preparation of the clean Pt(001) surface after film preparations required numerous sputtering-annealing cycles before LEED patterns start to show “hex”-reconstruction of Pt(001), which is characteristic of a clean surface.

Figure 1c–f shows LEED patterns and STM images of relatively “thick” CaO(001) films annealed at 1000 and 1200 K, respectively. Titration of the Pt atoms by CO revealed $<3\%$ of the sample area that might be uncovered. Clearly, UHV annealing at high temperatures leads to a better film ordering as the diffraction spots become considerably sharper. The film morphology studied by STM bears close similarity to the films grown on Mo(001).^{16,18} In both cases, relatively large, atomically flat terraces having step edges primarily running along the main crystallographic orientations of CaO(001) are observed. Note that there are also substantial amounts of screw

dislocations in the prepared films. Atomic size depressions about 1 Å in depth (see inset in Figure 1f) randomly distributed on terraces can tentatively be assigned to the point-like defects. It appears that the morphology of the CaO(001) films is almost independent on the lattice constant of a metal substrate underneath [2.77 Å on Pt(001) vs 3.15 Å on Mo(001)].

Large-scale STM images showed CaO(001) films uniformly covering a metal substrate. However, some “holes” in the films were observed showing a hexagonal superstructure with an ~ 10 Å periodicity. Although atomic resolution was not achieved, such areas could readily be scanned with a low tunneling bias (0.5 V), whereas the regular film surface typically required much higher biases, in the range of 3–4 V because CaO is an electric insulator. These findings allow us to assign such domains to an ultrathin CaO_x layer. Yet, the atomic structure remains unknown, such areas were minority.

3.2. TPD Results: Low Coverage. Figure 2a shows TPD spectra recorded on the CaO(001)/Pt(001) films as a function

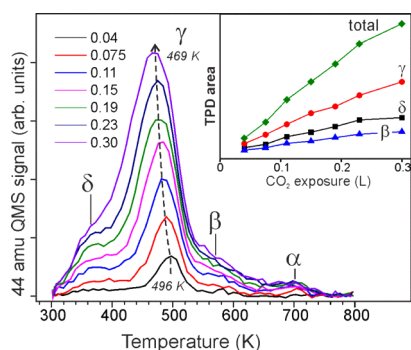


Figure 2. TPD spectra of CO₂ adsorbed at 300 K on a CaO(001)/Pt(001) film prepared at 1150 K. CO₂ exposures (in L) are indicated. The inset shows a total CO₂ uptake and signal area of each desorption state as a function of CO₂ exposure.

of CO₂ exposure up to 0.3 L (1 L = 10⁻⁶ Torr × s). In these experiments, CO₂ was dosed by backfilling the UHV chamber to 5×10^{-9} mbar. In order to minimize morphological changes, which may be induced by numerous TPD runs to elevated temperatures, the samples were only heated to 800 K. The original LEED pattern remains almost unchanged after tens of adsorption/desorption cycles, thus indicating no film restructuring in our conditions. As metallic Pt does not adsorb

CO₂ at room temperature, all desorption features in TPD spectra must be attributed to adsorption on CaO.

Several desorption states can be identified in spectra, which are labeled in Greek starting from the highest desorption temperature. The α peak rapidly saturates and may even be present by reaction with residual CO₂ during sample cooling. We assigned the α state to adsorption on yet poorly defined defects. (Interestingly, this peak was not observed on CaO(001) films grown on Mo(001), see below.) The spectra are dominated by the γ peak which gradually shifts from 496 to 469 K with increasing coverage. Two other desorption states (β centered at 390 K, and δ —at 560 K) appear as the shoulders to the γ peak. The peak areas of the β , γ , and δ states obtained by spectral deconvolution are plotted in the inset in Figure 2 as a function of CO₂ exposure together with the total uptake, which are all increasing in this coverage regime. Comparison of CO₂ desorption spectra measured on the same film sequentially annealed to 1100, 1150, and 1200 K in UHV showed no big differences in spectral evolution in this coverage regime.

In principle, the observed coverage-dependent shift of the peak maximum to the lower temperatures may be indicative of a second-order (recombinative) desorption kinetics that would imply CO₂ dissociation. However, this seems to be hardly possible on well-ordered stoichiometric CaO(001) surfaces at pressures applied. In addition, blank experiments with pure CO did not reveal its adsorption on our films. Therefore, CO would desorb immediately upon formation, and the surface recombination reaction would be impossible, if CO₂ could dissociate toward CO during exposure at 300 K. In another case of CO₂ decomposition up to elementary carbon, carbon deposits would result in continuous modification of the surface and hence nonreproducibility of the TPD results, which is not the case. Therefore, CO₂ dissociation can safely be excluded. Instead, the TPD spectra suggest nondissociative adsorption, with a peak shifting due to coverage effects.

Using a well-known Redhead analysis²⁰ of the first-order desorption kinetics using a typical prefactor 10¹³ s⁻¹, one can calculate the desorption energies. For the γ peak, it decreases from 129 to 122 kJ/mol with increasing CO₂ coverage. Accordingly, the estimates of the desorption energies for the α , β , and δ states yield 185 kJ/mol (700 K), 150 kJ/mol (570 K), and 100 kJ/mol (360 K), respectively. Utilizing the prefactor 10¹⁵ s⁻¹ in calculations results in all desorption energies increased by ~ 15 kJ/mol.

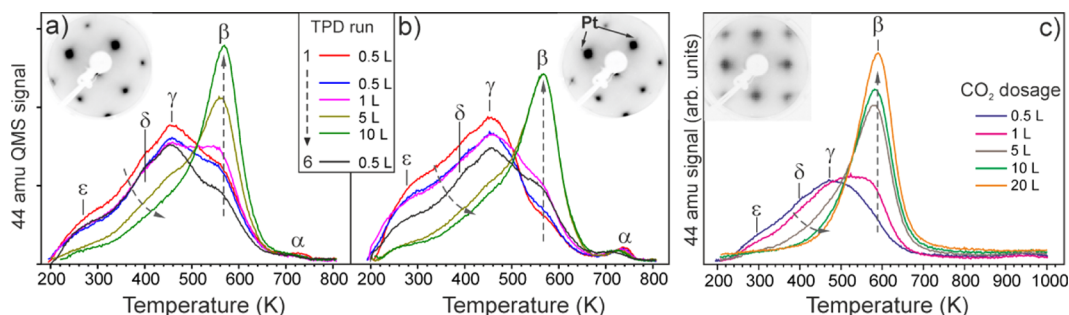


Figure 3. TPD spectra of CO₂ adsorbed on a CaO(001)/Pt(001) film annealed at 1100 K (a), and the film annealed at 1200 K (b). The sequence of TPD runs (from 1 to 6) and dosages are indicated. Arrows highlight general trend in spectral evolution upon increasing dosage. (c) Series of TPD spectra of CO₂ adsorbed on a CaO(001)/Mo(001) film at increasing exposure as indicated. Insets show LEED patterns (in negative contrast) of the films studied. The film studied in panel (b) also showed diffraction spots of Pt(001) as indicated by the arrows.

On the basis of our previous DFT and IRAS study¹⁸ focused on initial stages of CO₂ adsorption on CaO(001), we can tentatively assign the α state to adsorption on structural defects, whereas the principal γ peak reflects CO₂ adsorption on terrace sites as monodentate carbonates. Following the formation of surface aggregates (like pairs and chains predicted by DFT), CO₂ binding becomes weaker at increasing coverage.

3.3. TPD Results: High Exposures. TPD experiments of CO₂ adsorption on CaO(001) at high exposures were performed in another chamber using a directional doser. In order to minimize desorption signals from a weakly bonded CO₂ “multilayer” (see Figure S3) that may obscure the chemisorbed states, CO₂ was dosed at 220 K.

Figure 3a,b shows two sets of TPD spectra obtained for a dense CaO(001) film prepared at 1100 K (a) and for a thinner film prepared at 1200 K, which additionally showed diffraction spots of Pt(001)-(1 × 1) (b). The experiments were carried out as follows. First, the films were several times exposed to 0.5 L CO₂ in order to examine data reproducibility. Then, the dosage was stepwise increased to 1, 5, and 10 L. Finally, the sample was again exposed to 0.5 L to compare with the first TPD runs at the same exposure. The spectra on these two films look very similar, although the α peak seems to be more pronounced on a thinner film. Apparently, another low-temperature desorption state exists at around 280 K (labeled ϵ). Nonetheless, the spectra at low exposures (<0.5 L) are still dominated by the γ peak.

Drastic spectral changes occur at higher exposures: the β peak strongly gains in intensity, whereas the low-temperature signals attenuate, although the total CO₂ uptake does not change considerably, thus leading to the isosbestic point at around 500 K. The same behavior was observed for the CaO(001) films grown on Mo(001), as depicted in Figure 3c. (A full dataset is presented in Figure S4 in the Supporting Information). Obviously, any structural changes caused by consecutive TPD runs can be ruled out because the last spectrum for 0.5 L well reproduces those measured before high dosage experiments.

As discussed above, the initial shift of the γ peak to the lower temperatures (Figure 1) reflects gradual weakening of the CO₂ binding at increasing coverage. Such a behavior is well documented in the literature for many adsorbates on metal and oxide surfaces. CO₂ that becomes more strongly bound at high dosages is unusual. Adsorption of CO₂ molecules on top of the carbonate ad-layer or clustering of CO₂ molecules into three-dimensional particles, as a possible scenario, would only result in further lowered desorption temperature as intermolecular bonds in solid CO₂ (“dry ice”) are weak, thus resulting in the desorption signal at ~150 K (see Figure S3). Therefore, the spectral evolution observed at high exposures cannot be assigned to pure coverage effects. Moreover, the CO₂ uptake seems to reach saturation, and the β state gains in intensity, in essence, at the expense of low-temperature states.

Bearing in mind that CaO readily reacts with water, we examined possible effects of traces of water in the UHV background on CO₂ adsorption. In principle, surface “contamination” with water was thought to be unavoidable even under UHV conditions in experiments with polycrystalline CaO films on Si.¹³

Figure 4a shows desorption traces of CO₂ (44 amu) and H₂O (18 amu) in four TPD runs, all recorded upon exposure of 0.5 L CO₂ at 220 K. Note that cooling the sample down to 220 K after thermal flash usually takes a few minutes.

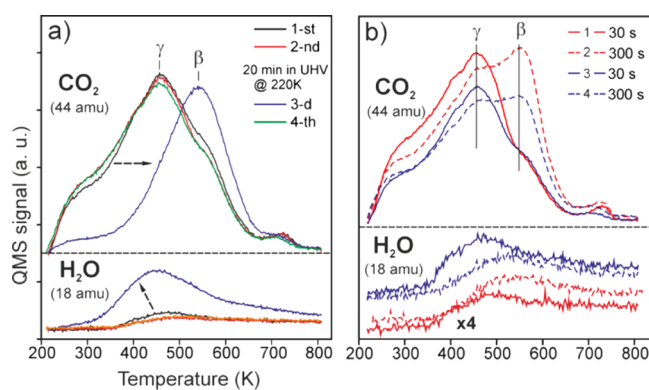


Figure 4. Repeated (1–4) TPD spectra of 0.5 L CO₂ exposed to a CaO(001)/Pt(001) film at 220 K. 44 amu (CO₂) and 18 amu (H₂O) signals are shown. In panel (a), between the 2nd and 3rd spectra, the sample was kept in UHV for 20 min prior to the CO₂ exposure. In panel (b), the spectra were recorded at two exposure times, 30 and 300 s, as indicated. Note, the 18 amu (H₂O) signal is here enlarged by a factor of 4, and the spectra are offset for clarity.

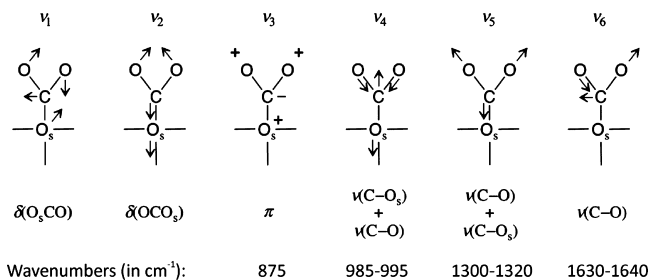
Comparison of the first two spectra indicates good reproducibility of desorption traces. At this exposure, the β state only manifests itself as a shoulder to the γ state. The amount of water desorbing between 400 and 500 K is negligible, thus suggesting that CO₂ is adsorbed on the clean CaO(001) surface. For the third run, the sample was kept at 220 K for 20 min prior to CO₂ dosing. It was thought that during this time, the sample will react with residual gases in the UHV background. This did cause dramatic effect on CO₂ desorption spectra which only showed the β state. Concomitantly, the amount of water desorbing from the CaO surface is substantially increased. (No other species were observed in the multimass spectra.) The fourth spectrum recorded immediately after the third one well reproduces the first two spectra, with the γ state dominating. These experiments show that the β state can be formed upon interaction of CO₂ with the CaO(001) surface “contaminated” with water ad-species. On the other hand, in TPD experiments shown in Figure 3, water molecules most likely interact with the surface already covered, at least partially, by monodentate carbonates first formed on the clean CaO(001) surface (see Figure 2). Nonetheless, the final effect is essentially the same: CO₂ desorption maximum shifts to much higher temperatures.

In another set of experiments, presented in Figure 4b, TPD spectra were measured for the same (0.5 L) exposures obtained either in 30 or 300 s exposure time by adjusting CO₂ pressure. Again, the spectra revealed considerable gain of the β peak intensity at the lower CO₂ flux. In principle, a longer exposure increases probability for water in the background to react with the surface. However, the observed difference in water desorption signals is not as obvious as in Figure 4a. Since both CO₂ and H₂O strongly adsorb onto the clean CaO(001) surface, there seems to be a competition for adsorption sites which result in complex kinetics.

3.4. IRAS Results. To gain information on the nature of ad-species formed during CO₂ adsorption at high exposures, we employed IRAS. Scheme 1 illustrates vibrational modes of CO₂ identified from our previous IRAS and DFT study¹⁸ of the initial stages of adsorption on the clean surfaces.

The most pronounced band at 1300–1320 cm⁻¹ is associated with symmetric stretching (ν_5) of monodentate carbonate (CO₃²⁻). The ν_4 mode shows up as a relatively weak

Scheme 1. Vibrational Modes and Experimentally Observed¹⁸ Frequencies for Monodentate Carbonate on the CaO(001) Surface; O_s Denotes the Surface Oxygen Atom



band at 965–990 cm^{-1} . According to the surface selection rules applied to IRAS stating that those vibrational modes that have a component of their dipole change perpendicular to the surface can be detected,²¹ the ν_3 and ν_6 modes are not observable on CaO(001) films, but on CaO nanoparticles exposing facets randomly oriented with respect to the metal surface plane.¹⁸ The frequencies of the bending modes (ν_1 and ν_2) are below the cutoff frequency of our setup and cannot be measured precisely.

Figure 5 displays the $\nu(\text{OH})$ stretching region (3300–3800 cm^{-1}) in addition to the 800–1800 cm^{-1} region, which is

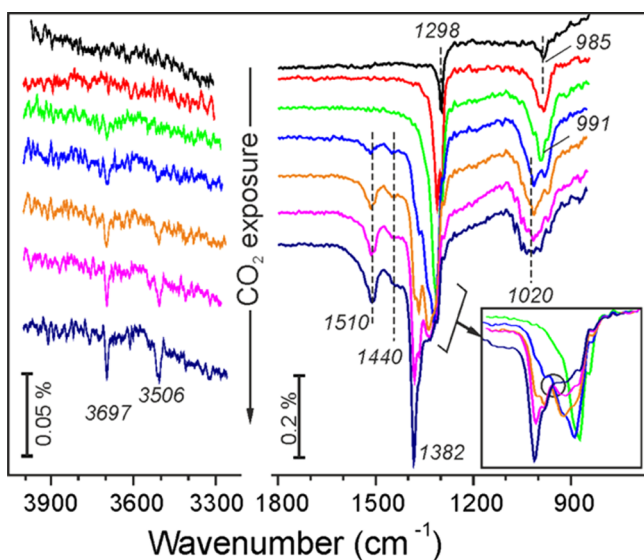


Figure 5. IRA spectra of CO_2 adsorbed at 300 K onto the CaO(001)/Mo(001) film at increasing coverage until saturation (~ 20 L). The spectra are offset, for clarity. The inset zooms in the 1300–1400 cm^{-1} region to highlight the isosbestic point (a circle).

associated with vibrations of adsorbed CO_2 . At low CO_2 exposures, only the ν_4 and ν_5 modes are detected. Their shift to higher frequencies (from 1298 to 1310 cm^{-1} , see the first three spectra) nicely correlates with the shift of the γ peak in TPD spectra (Figure 2) and can, therefore, be explained by increased density of monodentate carbonate species accompanied by their aggregation into pairs and linear chains as predicted by DFT.¹⁸

However, at further increasing CO_2 dosage, new bands at 1366 and 1382 cm^{-1} grow up, whereas the bands at 1310 and 1320 cm^{-1} attenuate, thus resulting in the isosbestic point (inset in Figure 5), that is, in a similar way observed during the $\gamma \rightarrow \beta$ transformation in TPD spectra (Figure 3). The ν_4 band

at around 990 cm^{-1} becomes broader and shifts to 1020 cm^{-1} basically following the blue shift of the ν_5 band. Last, a new band grows at 1510 cm^{-1} , and a small feature appears at 1440 cm^{-1} . Importantly, these changes occur simultaneously with the appearance and growth of sharp $\nu(\text{OH})$ bands at 3697 and 3506 cm^{-1} . Adsorption of isotopically labeled C^{18}O_2 onto the CaO(001) film (Figure S5 in the Supporting Information) led to all CO_2 related bands shifting to lower frequencies as anticipated on the basis of the reduced mass analysis, but not the $\nu(\text{OH})$ bands, again appearing at high C^{18}O_2 dosages. This finding indicates that hydroxyl species originate from adsorption of residual water in the UHV background rather than as impurity in CO_2 (expected to be isotopically labeled with the same O as CO_2). In any case, combined TPD and IRAS results provide compelling evidence that adsorption of CO_2 on the CaO(001) surface is affected even by traces of water in the ambient, the fact that has to be taken into account while discussing CO_2 adsorption on the “clean” surfaces and making comparison with theoretical calculations used for proper description of experimentally observed infrared bands.

Water adsorption on CaO was subject of numerous, both theoretical and experimental, studies using in particular IR spectroscopy. For example, the 3695 cm^{-1} band that closely resembles the 3697 cm^{-1} peak in our spectra was observed on CaO powders formed by high-temperature degassing of $\text{Ca}(\text{OH})_2$.²² This band has been assigned to a “free” hydroxyl to differentiate it from a “bound” hydroxyl that appears a considerably broader band centered at 3550 cm^{-1} . Recently, water adsorption has also been studied on the CaO(001)/Mo(001) films using IRAS, XPS, and STM, in combination with DFT.^{23,24} Two $\nu(\text{OD})$ bands were detected upon D_2O adsorption at 300 K: a sharp peak at 2725 cm^{-1} (3703 cm^{-1} for OH counterpart²²) and a broad one centered at ~ 2600 (3516) cm^{-1} . On the basis of the DFT calculations, the high-frequency band was assigned to O_wD species, where the subscript (w) denotes oxygen in dissociated water. Accordingly, the low-frequency band was assigned to O_sD hydroxyls, where the subscript (s) designates surface oxygen in the oxide. Note, however, that calculated values for the second band could only agree with the experimental ones in model structures containing at least 4 water molecules per CaO(001)-(3 \times 4) unit cell.²⁴ Therefore, we assign the $\nu(\text{OH})$ bands observed in CO_2 adsorption experiments at high dosages to hydroxyl species formed directly on the CaO(001) surface. Some deviation from the spectra obtained for pure water adsorption likely originates from that water adsorbs onto the carbonate precovered surface, not clean. In particular, the low-frequency band (3506 cm^{-1}) is much narrower, thus pointing to isolated OH species lacking H-bonds.

To gain further information about the role of water in CO_2 adsorption, the sample saturated with CO_2 at room temperature was dosed with D_2O at 300 K (Figure 6). (Note that the 3000–3450 cm^{-1} region is usually obscured by continuous H_2O adsorption on the cold IR detector, which is one of the reasons of using D_2O instead of H_2O in water adsorption IR measurements.) The results show that OH species undergo H–D exchange with D_2O : the $\nu(\text{OH})$ bands at 3697 and 3506 cm^{-1} disappear, whereas the $\nu(\text{OD})$ bands appear at 2733 and 2573 cm^{-1} . Concomitantly, the 1382 cm^{-1} peak is strongly reduced, whereas the 1510 and 1440 cm^{-1} bands gain in intensity. Again, spectral changes in this region show the isosbestic point (see inset). In addition, a broad band at ~ 1020

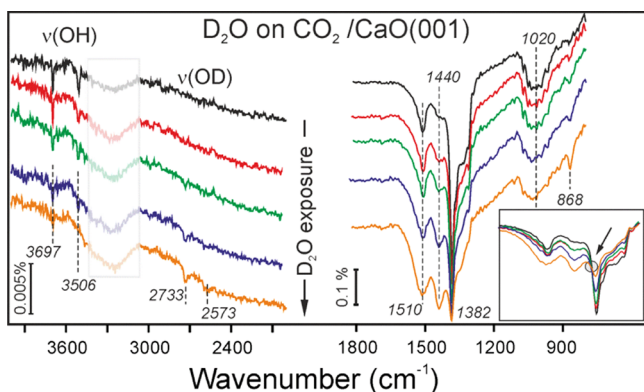


Figure 6. IRA spectra obtained at room temperature on the CaO(001)/Mo(001) film first saturated with CO₂ at 300 K (black curve) and then dosed with D₂O. (A continuously growing signal in the shaded 3000–3450 cm⁻¹ region is due to water adsorption in the IR detector.) The spectra are offset for clarity. The inset highlights the formation of isosbestic point.

cm⁻¹ attenuates, following the behavior of the 1382 cm⁻¹ peak, and a new sharp peak appears at 868 cm⁻¹.

The same kind of experiment performed on the CaO(001) surface first exposed to isotopically labeled CO₂¹⁸ revealed a similar behavior (Figure 7). Upon the H–D exchange, the

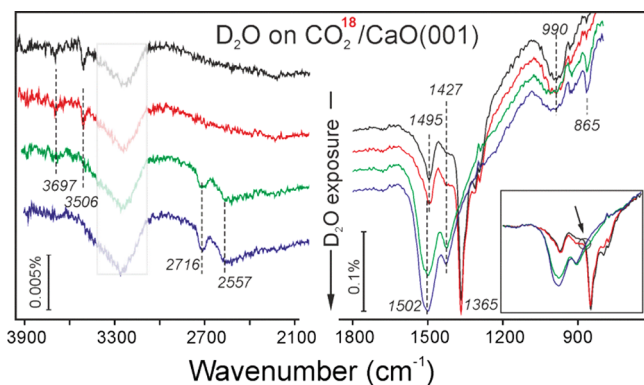


Figure 7. IRA spectra obtained at 300 K from the sample first saturated with CO₂¹⁸ (black curve) and then dosed with D₂O. (The shaded 3000–3450 cm⁻¹ region is affected by water adsorption in the IR detector.) The spectra are offset for clarity. The inset highlights the isosbestic point.

band at 1365 cm⁻¹ is strongly reduced, whereas the 1495 and 1427 cm⁻¹ bands gain in intensity, although the relative ratio is different from their CO₂¹⁶ counterparts (Figure 6). Again, a sharp band appears at 865 cm⁻¹. However, a closer look revealed both $\nu(\text{OD})$ bands red shifted by about 17 cm⁻¹ as compared to OD bands observed in experiments with CO₂¹⁶ (2716 and 2557 cm⁻¹ vs 2733 and 2573 cm⁻¹, see direct comparison in Figure S6 in the Supporting Information). This shift corresponds to oxygen exchange in surface hydroxyls (e.g., O¹⁶D vs O¹⁸D).^{25,26} Therefore, the H–D exchange is accompanied by O¹⁶–O¹⁸ exchange. Since the latter is only present in CO₂¹⁸ ad-species, the following surface reaction seems to occur: 2O¹⁶H + CO₂¹⁸ + D₂O¹⁶ (gas) → 2O¹⁸D + CO₂¹⁶ + H₂O¹⁶ (gas). Indeed, the principal band at 1365 cm⁻¹ associated with CO₂¹⁸ almost vanishes upon D₂O adsorption (Figure 7), whereas the CO₂¹⁶-related band at 1382 cm⁻¹ attenuates to a lesser extent (Figure 6). [Moreover, this

reaction may explain the relative increase and the blue shift of the 1495 cm⁻¹ band (see Figure 7) as it has now strong contribution from newly formed CO₂¹⁶ species.] Certainly, the process resulting in oxygen scrambling and H–D exchange involves a complex reaction of water with ad-layer containing both hydroxyl and carbonates species and yet remains poorly understood.

All in all, the IRAS results show no evidence for the bicarbonate (CO₃H⁻) formation in our conditions. Indeed, all bands observed in the 1600–800 cm⁻¹ region still belong to vibrations in CO₃²⁻. No new bands appear in this region upon H–D exchange observed in Figures 6 and 7, which could otherwise be associated with vibrations in COH entities in bicarbonates which strongly shift upon replacing H with D.²⁷ On the other hand, a very sharp band at 868 (865) cm⁻¹ in the above-presented experiments is very close in frequency to the π -band of monodentate carbonates (875 cm⁻¹, see Scheme 1), which was observed on CaO particles¹⁸ and not on the CaO(001) films solely because of the surface selection rules in IRAS.²¹ To gain more information on this issue, we performed additional IRAS experiments on a granular CaO film consisting of small particles (about 5 nm in size, see the inset in Figure 8) prepared on Ru(0001).

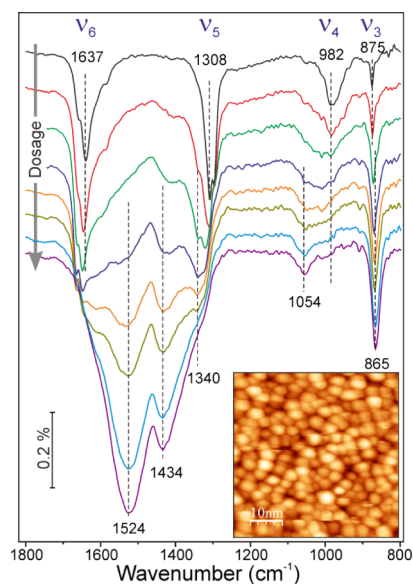


Figure 8. Selected IRA spectra of CO₂ adsorbed onto a granular CaO film grown on Ru(0001) at increasing coverage up to saturation at 300 K. STM image (50 nm × 50 nm) is shown in inset. The spectra are offset, for clarity.

As oxide surfaces are randomly oriented with respect to the metal plane, all ν_3 – ν_6 bands associated with monodentate carbonate formed at low CO₂ coverage can be detected (Figure 8). With increasing CO₂ dosage, first the band at 1340 cm⁻¹ and then the bands at 1434 and 1524 cm⁻¹ gain in intensity, whereas all bands characteristic for low coverage regime are strongly reduced (see also Figure S7a in the Supporting Information). In addition, a small signal shows up at 1054 cm⁻¹ together with a sharp band at 865 cm⁻¹ which is very close to the original 875 cm⁻¹ band, and it is difficult to conclude whether the latter remains or not. The $\nu(\text{OH})$ region did not show any evidence of the isolated hydroxyls (Figure S7b in the Supporting Information) as observed on a

CaO(001) film (Figure 5). It seems likely that such bands strongly overlap because of surface heterogeneity of CaO nanoparticles, resulting in a broad band which is, in addition, obscured by water adsorption signal in IR detector and hence difficult to resolve.

In principle, all bands in the last spectra presented in Figure 8 bear close similarity to those obtained in Figures 5–7, except their relative intensity. A considerably lower intensities of 1510, 1440, and 868 cm^{-1} bands on a CaO(001) film as compared to that of CaO particles (1524, 1444, and 865 cm^{-1} , respectively) can readily be explained by the surface selection rules. Since these bands develop upon adsorption of H_2O (Figure 5) as well as D_2O (Figures 6 and 7), we may conclude that the respective CO_2 -related species do not involve H (D) and hence cannot be assigned to bicarbonate (HCO_3^-). On the other hand, the bands appear simultaneously with surface hydroxyls, most clearly seen on CaO(001) films. Assuming that a sharp band at 865 cm^{-1} has the same (ν_3) character as of a monodentate carbonate (875 cm^{-1}), it can only be observed on the CaO(001) film surface if the carbonate plane is tilted with respect to the surface normal as a result of interaction with hydroxyl species in proximity. Moreover, this interaction would also affect the ν_5 and ν_6 vibrational modes, both the frequency and the intensity.

Finally, to link the IRAS and TPD results, we measured IRA spectra after dosing 10 L CO_2 at 110 K and thermal flash to specified (stepwise increasing) temperature. For clarity, Figure 9 only shows the spectra obtained after heating above 200 K to

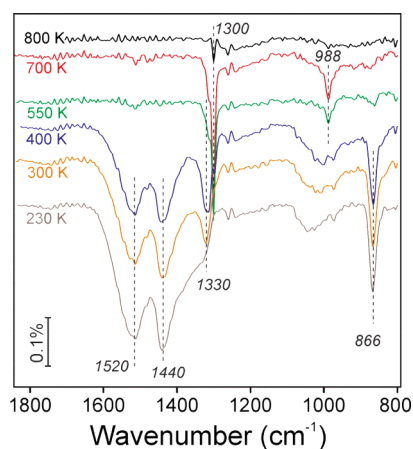


Figure 9. IRA spectra measured on the CaO(001)/Mo(001) film first exposed to 10 L of CO_2 at 110 K and then flashed to the stepwise-increased temperatures as indicated. All spectra were recorded at 110 K and are offset for clarity.

desorb physisorbed CO_2 molecules having a well-known IR fingerprint at around 2360 cm^{-1} . Note that some readsorption may occur during sample cooling. In addition, the temperature readings in the IRAS setup may deviate from those in TPD experiments and should be used as a guideline only.

Basically, the spectra change in reverse sequence to that observed upon increasing CO_2 dosage (compare to Figure 5), suggesting CO_2 adsorption to be fully reversible under the conditions studied. At 230 K, the 1520, 1440, and 866 cm^{-1} bands dominate the spectrum; the band at $\sim 1330 \text{ cm}^{-1}$ is only present as a shoulder. Upon heating to higher temperatures, all of the former bands attenuate and ultimately disappear, while the 1320 and 1300 cm^{-1} bands first gain in intensity, but then

disappear due to CO_2 desorption. The observed spectral evolution is fully consistent with the above-mentioned hypothesis that surface hydroxyls do not change the carbonate nature of CO_2 ad-species, but cause their reorientation (e.g., tilting). In fact, attenuation and final disappearance of the bands in the 1400–1500 cm^{-1} region on heating reflects the desorption of water (see Figures 4 and S4 in the Supporting Information) before CO_2 starts to desorb. Overall, water ad-species shows stabilizing effect on CO_2 binding to the CaO(001) surface.

4. CONCLUSIONS

Well-ordered CaO(001) films grown on Pt(001) and Mo(001) single crystals were used to study CO_2 adsorption by TPD and IRAS. The results show that CO_2 first adsorbs as monodentate carbonate (CO_3^{2-}), with the adsorption energy of 125 kJ/mol which decreases to 100 kJ/mol at increasing coverage due to agglomeration of carbonates in pairs and chains as predicted by DFT. However, at high exposures, CO_2 was found to desorb at considerably higher temperatures corresponding to adsorption energy of 147 kJ/mol. Analysis of TPD and IRA spectra revealed a critical role of residual water in the UHV background on CO_2 interaction with CaO. It is found that water molecules readily dissociate within the carbonate ad-layer formed at room temperature. Comparative IRAS study of CaO nanoparticles favors the model, where surface hydroxyls coexist with carbonate species and affect their adsorption geometry rather than form bicarbonate species. Therefore, surface hydroxyls show the stabilizing effect on the carbonate layer. Yet, theoretical calculations remain to be done to examine such scenario.

The results highlight the fact that even traces of water in the ambient atmosphere has to be taken into account while discussing CO_2 adsorption onto the “clean” surfaces and making comparison with theoretical calculations used for proper description of experimentally observed IR bands.

■ ASSOCIATED CONTENT

Supporting Information

The Supporting Information is available free of charge on the ACS Publications website at DOI: 10.1021/acs.jpcc.8b11415.

LEED and Auger spectra of CaO(001) films prepared on Pt(001) as a function of annealing temperature; TPD spectra of CO_2 adsorbed at 100 K on CaO(001)/Mo(001) films; and full dataset of TPD and IRA spectra of CO_2 on CaO(001) films and CaO particles at high exposures (PDF)

■ AUTHOR INFORMATION

Corresponding Author

*E-mail: shaikhutdinov@fhi-berlin.mpg.de.

ORCID

Shamil Shaikhutdinov: 0000-0001-9612-9949

Hans-Joachim Freund: 0000-0001-5188-852X

Present Addresses

[†]Faculty of Chemical, Environmental and Biological Science Technology, Dalian University of Technology, Dalian 116024, China.

[‡]Suzhou Institute of Nano-Tech and Nano-Bionics, Chinese Academy of Sciences, Suzhou 215123, China.

Notes

The authors declare no competing financial interest.

ACKNOWLEDGMENTS

The authors acknowledge Cluster of Excellence UNICAT administered by TU Berlin and Fonds der Chemischen Industrie for financial support. Y.C. acknowledges the Alexander von Humboldt Foundation for a fellowship.

REFERENCES

- (1) Centi, G.; Quadrelli, E. A.; Perathoner, S. Catalysis for CO₂ conversion: A Key Technology for Rapid Introduction of Renewable Energy in the Value Chain of Chemical Industries. *Energy Environ. Sci.* **2013**, *6*, 1711–1731.
- (2) Grasa, G.; González, B.; Alonso, M.; Abanades, J. C. Comparison of CaO-Based Synthetic CO₂ Sorbents under Realistic Calcination Conditions. *Energy Fuels* **2007**, *21*, 3560–3562.
- (3) Choi, S.; Drese, J. H.; Jones, C. W. Adsorbent Materials for Carbon Dioxide Capture from Large Anthropogenic Point Sources. *ChemSusChem* **2009**, *2*, 796–854.
- (4) Wang, S.; Yan, S.; Ma, X.; Gong, J. Recent Advances in Capture of Carbon Dioxide Using Alkali-metal Based oxides. *Energy Environ. Sci.* **2011**, *4*, 3805–3819.
- (5) Fukuda, Y.; Tanabe, K. Infrared Study of Carbon Dioxide Adsorbed on Magnesium and Calcium Oxides. *Bull. Chem. Soc. Jpn.* **1973**, *46*, 1616–1619.
- (6) Pacchioni, G.; Ricart, J. M.; Illas, F. Ab Initio Cluster Model Calculations on the Chemisorption of CO₂ and SO₂ Probe Molecules on MgO and CaO (100) Surfaces. A Theoretical Measure of Oxide Basicity. *J. Am. Chem. Soc.* **1994**, *116*, 10152–10158.
- (7) Jensen, M. B.; Pettersson, L. G. M.; Swang, O.; Olsbye, U. CO₂ Sorption on MgO and CaO Surfaces: A Comparative Quantum Chemical Cluster Study. *J. Phys. Chem. B* **2005**, *109*, 16774–16781.
- (8) Freund, H.-J.; Roberts, M. W. Surface Chemistry of Carbon Dioxide. *Surf. Sci. Rep.* **1996**, *25*, 225–273.
- (9) Taifan, W.; Boily, J.-F.; Baltrusaitis, J. Surface Chemistry of Carbon Dioxide Revisited. *Surf. Sci. Rep.* **2016**, *71*, 595–671.
- (10) Burghaus, U. Surface Science Perspective of Carbon Dioxide Chemistry—Adsorption Kinetics and Dynamics of CO₂ on Selected Model Surfaces. *Catal. Today* **2009**, *148*, 212–220.
- (11) Doyle, C. S.; Kendelewicz, T.; Carrier, X.; Brown, G. E. The Interaction of Carbon Dioxide With Single Crystal CaO(100) surfaces. *Surf. Rev. Lett.* **1999**, *06*, 1247–1254.
- (12) Kadossov, E.; Burghaus, U. Adsorption Kinetics and Dynamics of CO, NO, and CO₂ on Reduced CaO(100). *J. Phys. Chem. C* **2008**, *112*, 7390–7400.
- (13) Voigts, F.; Bebensee, F.; Dahle, S.; Volgmann, K.; Maus-Friedrichs, W. The Adsorption of CO₂ and CO on Ca and CaO Films Studied With MIES, UPS and XPS. *Surf. Sci.* **2009**, *603*, 40–49.
- (14) Ochs, D.; Braun, B.; Maus-Friedrichs, W.; Kempter, V. CO₂ Chemisorption at Ca and CaO surfaces: A study With MIES, UPS(HeI) and XPS. *Surf. Sci.* **1998**, *417*, 406–414.
- (15) Shao, X.; Myrach, P.; Nilius, N.; Freund, H.-J. Growth and Morphology of Calcium-Oxide Films Grown on Mo(001). *J. Phys. Chem. C* **2011**, *115*, 8784–8789.
- (16) Cui, Y.; Pan, Y.; Pascua, L.; Qiu, H.; Stiehler, C.; Kühlenbeck, H.; Nilius, N.; Freund, H.-J. Evolution of the Electronic Structure of CaO Thin Films Following Mo Interdiffusion at High Temperature. *Phys. Rev. B: Condens. Matter Mater. Phys.* **2015**, *91*, 035418.
- (17) Cui, Y.; Shao, X.; Baldofski, M.; Sauer, J.; Nilius, N.; Freund, H.-J. Adsorption, Activation, and Dissociation of Oxygen on Doped Oxides. *Angew. Chem., Int. Ed.* **2013**, *52*, 11385–11387.
- (18) Solis, B. H.; Cui, Y.; Weng, X.; Seifert, J.; Schauermaier, S.; Sauer, J.; Shaikhutdinov, S.; Freund, H.-J. Initial Stages of CO₂ Adsorption on CaO: A Combined Experimental and Computational Study. *Phys. Chem. Chem. Phys.* **2017**, *19*, 4231–4242.
- (19) Solis, B. H.; Sauer, J.; Cui, Y.; Shaikhutdinov, S.; Freund, H.-J. Oxygen Scrambling of CO₂ Adsorbed on CaO(001). *J. Phys. Chem. C* **2017**, *121*, 18625–18634.
- (20) Redhead, P. A. Thermal Desorption of Gases. *Vacuum* **1962**, *12*, 203–211.
- (21) Hollins, P.; Pritchard, J. Infrared Studies of Chemisorbed Layers on Single Crystals. *Prog. Surf. Sci.* **1985**, *19*, 275–349.
- (22) Low, M. J. D.; Takezawa, N.; Goodsel, A. J. Infrared study of hydroxyls on active CaO. *J. Colloid Interface Sci.* **1971**, *37*, 422–429.
- (23) Zhao, X.; Shao, X.; Fujimori, Y.; Bhattacharya, S.; Ghiringhelli, L. M.; Freund, H.-J.; Sterrer, M.; Nilius, N.; Levchenko, S. V. Formation of Water Chains on CaO(001): What Drives the 1D Growth? *J. Phys. Chem. Lett.* **2015**, *6*, 1204–1208.
- (24) Fujimori, Y.; Zhao, X.; Shao, X.; Levchenko, S. V.; Nilius, N.; Sterrer, M.; Freund, H.-J. Interaction of Water with the CaO(001) Surface. *J. Phys. Chem. C* **2016**, *120*, 5565–5576.
- (25) Zaki, E.; Mirabella, F.; Ivars-Barceló, F.; Seifert, J.; Carey, S.; Shaikhutdinov, S.; Freund, H.-J.; Li, X.; Paier, J.; Sauer, J. Water Adsorption on the Fe₃O₄(111) Surface: Dissociation and Network Formation. *Phys. Chem. Chem. Phys.* **2018**, *20*, 15764–15774.
- (26) Yu, X.; Emmez, E.; Pan, Q.; Yang, B.; Pomp, S.; Kaden, W. E.; Sterrer, M.; Shaikhutdinov, S.; Freund, H.-J.; Goikoetxea, I.; Włodarczyk, R.; Sauer, J. Electron Stimulated Hydroxylation of a Metal Supported Silicate Film. *Phys. Chem. Chem. Phys.* **2016**, *18*, 3755–3764.
- (27) Baltrusaitis, J.; Grassian, V. H. Surface Reactions of Carbon Dioxide at the Adsorbed Water–Iron Oxide Interface. *J. Phys. Chem. B* **2005**, *109*, 12227–12230.